35th Annual International Conference of the IEEE EMBS
Osaka, Japan, 3 - 7 July, 2013

Electromagnetic and Thermal Effects of IR-UWB Wireless Implant Systems on the Human Head

Kasun M.S. Thotahewa, *Student Member, IEEE* , Jean-Michel Redouté, *Member, IEEE,*

and Mehmet R.Yuce, *Member, IEEE*

***Abstract*— The usage of implanted wireless transmitting devices inside the human body has become widely popular in recent years. Applications such as multi-channel neural recording systems require high data rates in the wireless transmission link. Because of the inherent advantages provided by Impulse-Radio Ultra Wide Band (IR-UWB) such as high data rate capability, low power consumption and small form factor, there has been an increased research interest in using IR-UWB for bio-medical implant applications. Hence it has become imperative to analyze the electromagnetic effects caused by the use of IR-UWB when it is operated in or near the human body. This paper reports the electromagnetic effects of head implantable transmitting devices operating based on Impulse Radio Ultra Wide Band (IR-UWB) wireless technology. Simulations illustrate the performance of an implantable UWB antenna tuned to operate at 4 GHz with an -10dB bandwidth of approximately 1 GHz when it is implanted in a human head model. Specific Absorption Rate (SAR), Specific Absorption (SA) and temperature increase are analyzed to compare the compliance of the transmitting device with international safety regulations.**

I. INTRODUCTION

Physiological signal monitoring using implantable wireless devices has become increasingly popular recently [1-4]. With the emergence of new techniques to record physiological data such as neural recording systems [5], the need of high data rate wireless transmission has become a key requirement for implantable devices. Impulse Radio Ultra Wide Band (IR-UWB) can be identified as a technology which caters the need for high data rate while requiring low power consumption [6]. UWB signals are defined as signals having a fractional bandwidth larger than 0.2 or a bandwidth of at least 500 MHz. UWB is allowed to operate in the 0-960 MHz and 3.1-10 GHz bands with the effective isotopic radiated power (EIRP) kept below -41.3 dBm/MHz [7]. Figure 1 shows the use of IR-UWB to transmit data from a brain implant. With the extensive use of wireless devices within or at close proximity to the human body, electromagnetic effects caused by the interaction between radio frequency waves and human tissues are of paramount importance. Specific Absorption Rate (SAR), which determines the amount of signal energy absorbed by the human body tissue, is used as the index for many standards to regulate the amount of exposure of the human body to electromagnetic radiation [8-9].

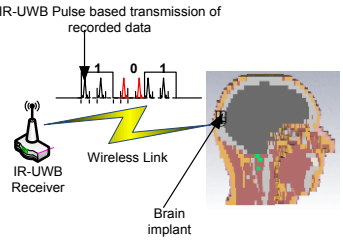

Fig. 1. Brain implant communication using IR-UWB.

As UWB communication becomes more prominent in high data rate implant communication [6, 10, 11], it is important to investigate the electromagnetic effects caused by a UWB transmitter implanted in the human body. Several publications are found in the literature that has analyzed the effect of UWB on the human body based on on-body scenarios [12-13]. While these results provide a general understanding about the electromagnetic effects caused by on-body propagation of UWB signals, the work in this article does not look into the effects caused by implanted UWB devices. Many reported studies used homogeneous human body models; hence they do not depict the differences in properties of various types of tissue materials which can significantly affect the results. Also it should be noted that the SAR variation depends on antenna properties such as directivity, orientation and gain. Few reported studies demonstrate the effects of radio frequency transmission from implantable devices inside the human body [14-16]. The work reported in [16] illustrates the SAR variation caused by an IR-UWB source inside the human stomach. However, it has not considered an antenna model in the simulations: additionally, the FCC regulations which govern the UWB indoor propagation are not taken into account. The work presented in [17] has analyzed the SAR variation inside the human head caused by the UWB signals, but has used a simple layered tissue model.

This paper presents the electromagnetic and thermal effects of IR-UWB transmission from a brain implant. We used a complex head model to simulate the combination of tissue materials present in the head. An implantable antenna working at UWB frequencies is used as the source of the UWB signals. An IR-UWB pulse, operating at a center frequency of 4 GHz and a bandwidth of 1GHz has been

• K.M. S. Thotahewa, M.R. Yuce and J.-M. Redouté are with the School of Electrical and Computer Systems Engineering at Monash University, Clayton, VIC, 3800, Australia. E-mail: kasun.thotahewa@monash.edu, Mehmet.Yuce@monash.edu,and jean-michel.redoute@monash.edu.

chosen as the excitation to the antenna. This range is selected so that the UWB spectrum has minimum interference from other wireless technologies such as 5 GHz Wi-Fi. The simulations are conducted in CST Studio [18], which has been recognized by the FCC as a suitable simulation tool for SAR calculations.

II. SAR, SA and Tissue Temperature Calculation Methods

A. SAR and SA

The SAR value for a certain material subjected to an electromagnetic field can be calculated by (1) [25].

$$\mathrm{SAR} = \frac{1}{2}\frac{\sigma}{\rho}|\mathrm{E}|^2 \quad (1)$$

,where E is the root mean square (RMS) electric field strength, ρ is the mass density (in kg/m^3), and σ is the conductivity of the tissue. The electric field is related to the complex relative permittivity by Maxwell's curl equations. Hence the SAR variation inherently depends on the relative permittivity of the material which itself depends on the incident frequency of the electromagnetic signal. Gabriel et al. has proposed a method of evaluating the frequency dependent relative permittivity of a material by the so called 4 - Cole Cole model approximation given in the equation below [19],

$$\varepsilon_r'(\omega) = \varepsilon_\infty + \sum_{n=1}^{4} \frac{\Delta\varepsilon_n}{1+(j\omega\tau_n)^{1-\alpha_n}} + \frac{\sigma_i}{j\omega\varepsilon_0} \quad (2)$$

,where j=$\sqrt{-1}$ is the imaginary unit, ω is the angular frequency, ε_∞ is the permittivity when $\omega \to \infty$ (permittivity in Terahertz frequencies in practical scenarios), $\Delta\varepsilon_n$ is the change in the permittivity in a specified frequency range during the nth iteration, τ_n is the relaxation time during the nth iteration, $\alpha_n$is the nth iteration of the distribution parameter which is a measure of the broadening of dispersion, σ_i is the static ionic conductivity and ε_0= 8.85×10^{-12} F/m is the permittivity of the free space. We used the 4- Cole Cole method to model the dielectric dispersion in the human body tissues used for the simulations in this paper. The parameter values required for this equation are taken from the values given in [19].

Apart from the frequency dependent dispersive nature of the tissue materials, the human age affects the electromagnetic behavior of body tissues. This is mainly due to the change in the water content of tissue with age. We followed the methods provided in [20] in order to calculate the age related human tissue properties. We assumed that the age of the human head model used for the simulations to be 35 years old. By using the 4-Cole Cole approximation in combination with the age related tissue parameter approximations it is possible to characterize the human tissue properties with sufficient precision.

The Finite Integration Technique (FIT) is used as the volume discretization approach for the described simulations. This technique is used to calculate the absorption loss of the body tissues by discretizing the Maxwell's curl equations in a specified domain [21]. The discretizing volume element is chosen to be cubic, and appropriate boundary conditions are applied in order to define the power absorbed within that cube. Present simulations use an IR-UWB signal pulse as the excitation signal, and are conducted in order to calculate the 10g averaged SAR so as to compare it with the ICNIRP specifications for pulse transmission [8].

The Specific Absorption (SA) per pulse, which is being used to introduce additional limitations for pulsed transmissions in the ICNIRP limitations, is computed using;

$$SA = SAR \times T_p \quad (3)$$

,where T_p is the pulse duration.

B. Temperature Variation

When exposed to an electromagnetic field, the absorbed power by the body tissues causes a temperature increase. A temperature increase exceeding 1-2 ^{o}C in the human body tissue can cause adverse health effects such as a heat stroke [22]. In addition to the study of SAR variations, this paper also analyses the temperature variation in the human head, when it is exposed to IR-UWB transmission from an implanted transmitter. The temperature of the body tissues is modeled using the bio heat equation in (4) [23].

$$\mathrm{Cp}\frac{\delta \mathrm{T}}{\delta \mathrm{t}} = \nabla.(\mathrm{k}\nabla\mathrm{T}) + \rho.\mathrm{SAR} + \mathrm{A} - \mathrm{B}(\mathrm{T} - \mathrm{T_b}) \quad (4)$$

,where K is the thermal conductivity, ρ is the mass density, Cp denotes the specific heat, A is the basal metabolic rate, B is the term associated with blood perfusion, ρ is the tissue density in $\frac{\mathrm{kg}}{\mathrm{m}^3}$and $\nabla.(k\nabla T)$ represents the thermal spatial diffusion term for heat transfer through conduction at temperature T in degrees Celsius.

III. Antenna Model

The variation of the SAR is highly dependent on the antenna parameters such as directivity and gain. The UWB antenna considered in this paper was modeled on the work presented in [24]. The dimensions of the antenna are 23.7×9×1.27 mm, which are reasonable values to be used within a neural implant. The antenna is tuned to operate at around 4 GHz with a bandwidth of 1 GHz, which fulfills the bandwidth requirement imposed by the FCC for UWB communication. The antenna was inserted inside a capsule shaped casing with a negligible thickness compared to the antenna dimensions, in order to prevent direct contact between antenna radiating elements and the neighboring tissue. Using an insulating material with a relative permittivity close to that of the surrounding tissue material between the latter and the antenna, increases the impedance matching characteristics [24]. Glycerin, which has a relative permittivity value of 50, is chosen as the appropriate insulating material when the antenna is surrounded mainly by the brain tissue which has a relative permittivity of around 40 at 4 GHz. The designed antenna is half embedded inside the insulating material, where only the lower half of the antenna is immersed in glycerin. This improves the impedance matching characteristics in the implant [24]. The antenna is placed at 6 mm distance from the surface of the head. Figure 2 depicts how this antenna model is used alongside the CST voxel head model in order to perform present simulations.

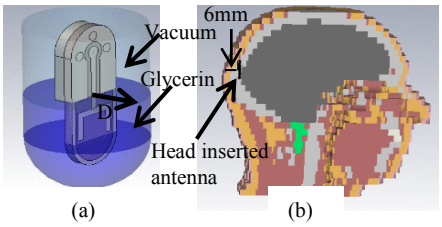

Fig.2. (a) IR-UWB antenna (b) Insertion in the head.

The gain and the S-parameters of the head implanted antenna are depicted in Figure 3 and Figure 4 respectively.

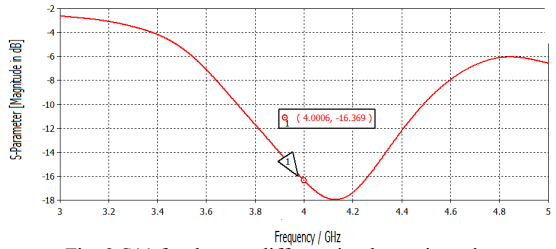

Fig. 3.S11 for the two different implant orientations.

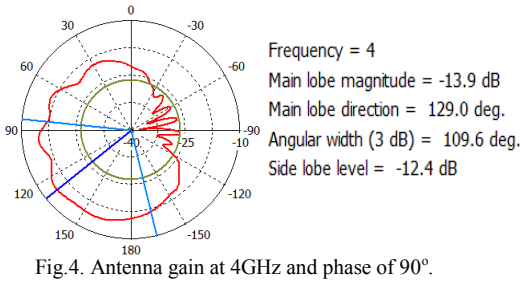

Fig.4. Antenna gain at 4GHz and phase of 90º.

An IR-UWB signal centered at 4 GHz with a bandwidth of 1 GHz has been applied to the designed UWB antenna. Initially, an FCC regulated IR-UWB pulse [7] has been used in order to investigate SAR and temperature effects. The use of an FCC regulated UWB pulse for excitation is useful to compare the obtained results with the results available in the literature. The pulse duration is 2 ns. These pulses are obtained from a pulse train with a period of 50 ns. The pulse amplitude of that signal has been adjusted ensuring that the input power to the antenna falls within the FCC regulated power spectrum.

IV. Results and Discussion

A. SAR and SA Variation

Using the developed simulation models, the 10g averaged SAR variations for three different input power values have been analyzed in a 35 year old adult head (Figure 2). Three simulation scenarios have been analyzed based on the input power to the antenna. The first scenario uses a FCC regulated IR-UWB pulse which lies within the specified -41.3dBm/MHz limit. The second scenario is obtained by considering the results in Figure 4 : it can be observed in Figure 4 that the resulting maximum antenna gain is -13.9dB. This means that if a pulse with a peak power limit of 13.9 dB higher than the FCC regulated peak power limit of -41.3 dBm/MHz is used as the input to the implanted antenna, the radiation in free space will lie at the FCC limit [24]. This corresponds to an input pulse with peak spectral limit of -27.4 dBm/MHz. The Specific Absorption (SA) for these two scenarios is also calculated for a pulse width of 2 ns, in order to form a comparison with the ICNIRP special regulations for pulse transmissions. In the third scenario, an IR-UWB pulse which causes a maximum SAR of 2W/kg is used: the latter value is specified as the maximum allowable SAR limit by the ICNIRP regulations. The results are depicted in Figure 5.

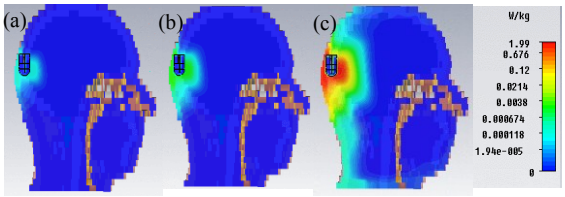

Max. SAR= 0.116 mW/kg. Max SA= 0.232pJ/kg

Max. SAR =2.43 mW/kg. Max SA= 4.86pJ/kg

Max. SAR =1.99 W/kg. Max SA= 3.98nJ/kg

Fig. 5. Side view of the 10g averaged SAR variation in the adult voxel head model for the peak spectral power limits of (a) -41.3dBm/MHz (b) -27.4 dBm/MHz and (c) 0.9dBm/MHz.

The results depicted in Figure 5 show that the SAR and SA values obtained for the first and second scenario are well within the ICNIRP regulation limit for a single pulse of 2W/kg and 2mJ/kg respectively. This is due to the very small power contained in the signal (a total in-band accepted power of 0.0024mW in scenario one and 0.0504mW in scenario two considering a bandwidth of 1 GHz). It should be noted that the color scale is set to reflect the maximum SAR in all the scenarios, and is logarithmically marked to yield an acceptable resolution for low SAR values. The results obtained in scenario two are comparable with the results reported in [25], where the authors have used the FCC regulated radiated power as the excitation source for calculating their SAR values. The obtained SAR results in this paper are comparatively higher than those reported in [25] since this paper considers an implanted transmitter, while [25] described an on-body circuit. The SAR variation in scenario three uses a signal which lies within a peak limit of 0.9 dBm/MHz for an amplitude increased version of the IR- UWB pulse, but violates the FCC regulations for IR-UWB indoor propagation.

B. Temperature Variation

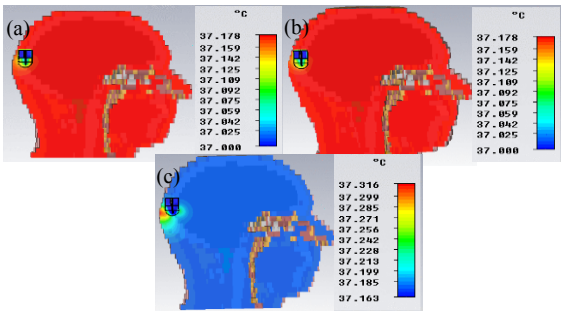

Fig. 6. Temperature variation for a signal with peak spectral power limits of (a) -41.3dBm/MHz (b) -27.4 dBm/MHz (c) 0.9 dBm/MHz. using bio heat equation.

Simulations using the same input power scenarios as reported in Figure 4(a-c) are used to obtain the

corresponding temperature variations. The bio heat equation considers the variation of basal metabolic rate and blood perfusion. Because of the short duration of the excitation pulse, the heat conduction which occurs through sweating is assumed to be negligible. The temperature increase is measured after the steady state is achieved. Figure 5 depicts the obtained temperature variations.

It can be seen in Figure 6 (a) and (b) that there is no temperature increase in the head for the corresponding signals. This is due to the generated temperature resulting from the small electric field being regulated by the blood perfusion inside the head. As can be observed in these two cases, the temperature in the immediate vicinity of the antenna is lower than the temperature of the surrounding tissue that is heated up by metabolic activities. This is because of the thermal absorption by glycerin surrounding the antenna. The temperature increase is clearly visible in Figure 6 (c) where a higher power signal is used for excitation.

V. CONCLUSION

This work describes the electromagnetic exposure effects of a UWB implanted device targeted at applications such as neural recording and brain computer interfaces. The FCC regulations for the outdoor transmit power for UWB communication determines the maximum allowable signal power from an implanted IR-UWB based transmitter. The SAR and SA results for the maximum peak power limits of -41.3 dBm/MHz and -27.4 dBm/MHz lie well within the ICNIRP regulated limits. The temperature increase due to the exposure of the head tissues to the IR-UWB electromagnetic field at those peak power limits is found to be well within the control of thermal regulatory mechanisms of the human body. Also, it was observed that the SAR is highly dependent on the bandwidth of the IR-UWB signal. It is found that a pulse with a peak power limit of 13.9 dB higher than the FCC regulated peak power can be utilized without violating SAR/SA limits, as well as the outdoor FCC regulations for this particular model.

REFERENCES

[1] N. Gopalsami, I. Osorio, S. Kulikov, S. Buyko, A.Martynov and A.C.Raptis,"SAW Microsensor Brain Implant for Prediction and Monitoring of Seizures," *IEEESensors Journal*, vol.7, no.7, pp.977-982, July 2007.

[2] A.V. Nurmikko, J.P. Donoghue, L.R. Hochberg, W.R. Patterson, Yoon-Kyu Song, C.W. Bull, D.A. Borton, F. Laiwalla, Sunmee Park, Yin Ming and J. Aceros, "Listening to Brain Microcircuits for Interfacing With External World,' Proceedings of the IEEEProgress in Wireless Implantable Microelectronic Neuroengineering Devices, vol.98, no.3, pp.375-388, March 2010.

[3] C. Cavallotti, M. Piccigallo, E. Susilo, P. Valdastri, A. Menciassi, Paolo Dario, An integrated vision system with autofocus for wireless capsular endoscopy, *Sensors and Actuators A: Physical,* vol.156, no.1,pp. 72-78, 2009.

[4] X. Chen,X. Zhang,L. Zhang,X. Li,N. Qi,H. Jiang,Z.Wang; , "A Wireless Capsule Endoscope System With Low-Power Controlling and Processing ASIC," *IEEE Transactions on Biomedical Circuits and Systems,* , vol.3, no.1, pp.11-22, Feb. 2009.

[5] F. Shahrokhi, K. Abdelhalim, D. Serletis, P.L. Carlen, andR. Genov, "The 128-Channel Fully Differential Digital Integrated Neural Recording and Stimulation Interface," *IEEE Transactions on Biomedical Circuits and Systems*, vol.4, no.3, pp.149-161, June 2010.[16]

[6] M. Chae, Z. Yang, M. R. Yuce, L. Hoang and W. Liu, "A 128-channel 6mW Wireless Neural Recording IC with Spike Feature Extraction and UWB Transmitter," IEEE Transactions on Neural Systems & Rehabilitation Engineering, vol. 17, pp. 312 - 321, August 2009.[17]

[7] FCC 02-48 (UWB FIRST REPORT AND ORDER), 2002.

[8] ICNRP, "Guidelines for Limiting to time varying electric, magnetic, and electromagnetic fields (up to 300 GHz)," International Commission on Non-Ionizing Radiation Protection, 1997.[5]

[9] Institute of Electrical and Electronics Engineers (IEEE), "'IEEE Standard for Safety Levels with Respect to Human Exposure to Radio Frequency Electromagnetic Fields, 3 kHz to 300 GHz'," IEEE, IEEE Std C95.1-2005, 2005.[6]

[10] O. Novak, C. Charles, andR.B. Brown, "A fully integrated 19 pJ/pulse UWB transmitter for biomedical applications implemented in 65 nm CMOS technology," 2011 IEEE International Conference on *Ultra-Wideband (ICUWB)*, pp.72-75, 14-16 Sept. 2011.10

[11] Wei-Ning Liu; Tsung-Hsien Lin; , "An energy-efficient ultra-wideband transmitter with an FIR pulse-shaping filter," *International Symposium on VLSI Design, Automation, and Test*, pp.1-4, 23-25 April 2012.11

[12] Z. N. Chen, A. Cai, T. S. P. See, X. Qing, and M. Y. W. Chia, "Small planar UWB antennas in proximity of the human head," IEEE Transactions on Microwave. Theory and Techniques, vol. 54, no. 4, pp. 1846–1857, Apr. 2006.

[13] C. Buccella, V. De Santis, and M. Feliziani, "Prediction of temperature increase in human eyes due to RF sources," *IEEE Transactions on Electromanetic.Compatibility*, vol. 49, no. 4, pp. 825–833, Nov. 2007.

[14] P. Soontornpipit, "Effects of Radiation and SAR from Wireless Implanted Medical Devices on the Human Body," *Journal of the Medical Association of Thailand*, vol.95, no.2, pp.189-197, 2012.7

[15] L. Xu, M.Q.H. Meng, H.Ren, and Y. Chan , "Radiation characteristics of ingestible wireless devices in human intestine following radio frequency exposure at 430, 800, 1200, and 2400 MHz," *IEEE Transactions on Antennas and Propagation,* vol.57, no.8, pp.2418-2428, Aug. 2009.8

[16] T. Koike-Akino, "SAR analysis in tissues for in vivo UWB body area networks," *IEEE Global Telecommunications Conference,* pp.1-6, Nov. 30 -Dec. 4 2009.21

[17] H. Bahrami, B. Gosselin, L.A.Rusch, "Realistic modeling of the biological channel for the design of implantable wireless UWB communication systems," *IEEE Annual International Conference of the Engineering in Medicine and Biology Society (EMBC)*, pp. 6015 – 6018, 2012.

[18] CST STUDIO SUITE™, CST AG, Germany, www.cst.com.23

[19] S. Gabriel, R. W. Lau, and C. Gabriel, "The dielectric Properties of Biological Tissues: III. Parametric Models for the Dielectric Spectrum of Tissues," *Physics in Medicine and Biology*, vol. 41, no. 11, pp. 2271–2293, 1996.14

[20] J. Wang, O. Fujiwara, S. Watanabe, "Approximation of aging effect on dielectric tissue properties for SAR assessment of mobile telephones," IEEE Transactions on Electromagnetic Compatibility, vol.48, no.2, pp. 408- 413, May 2006.

[21] T. Weiland, M. Timm, and I. Munteanu, "A practical guide to 3-D simulation*", IEEE Microwave Magazine*, vol. 9, no. 6, pp. 62-75, 2008.

[22] P. Bernardi, M. Cavagnaro, S. Pisa, E. Piuzzi, "Specific absorption rate and temperature elevation in a subject exposed in the far-field of radio-frequency sources operating in the 10-900-MHz range," *IEEE Transactions onBiomedical Engineering*, vol.50, no.3, pp.295-304, March 2003.

[23] H. H. Pennes, "Analysis of tissue and arterial blood temperatures in resting forearm," *J. Appl. Physiol.*, vol. 1, pp. 93–122, 1948.

[24] T. Dissanayake, K.P. Esselle, M.R. Yuce, "Dielectric Loaded Impedance Matching for Wideband Implanted Antennas," *IEEE Transactions on Microwave Theory and Techniques*, vol.57, no.10, pp.2480-2487, Oct. 2009.

[25] Q. Wang, and J. Wang, "SA/SAR analysis for multiple UWB pulse exposure," Asia-Pacific Symposium on *Electromagnetic Compatibility and 19th International Zurich Symposium on Electromagnetic Compatibility,* pp.212-215, 19-23 May 2008.